Current Biology 22, 1429–1434, August 7, 2012 ©2012 Elsevier Ltd All rights reserved DOI 10.1016/j.cub.2012.05.046

Report

Residual Attention Guidance in Blindsight Monkeys Watching Complex Natural Scenes

Masatoshi Yoshida,[1,2,6] Laurent Itti,[3,4,6,*] David J. Berg,[4] Takuro Ikeda,[1,7] Rikako Kato,[1] Kana Takaura,[1,2,8] Brian J. White,[5] Douglas P. Munoz,[5] and Tadashi Isa[1,2]

[1]Department of Developmental Physiology, National Institute for Physiological Sciences, Okazaki 444-8585, Japan
[2]School of Life Science, The Graduate University for Advanced Studies, Hayama 203-0193, Japan
[3]Computer Science Department
[4]Neuroscience Graduate Program
University of Southern California, Los Angeles, CA 90089, USA
[5]Centre for Neuroscience Studies, Queen's University, Kingston, ON K7L 3N6, Canada

Summary

Patients with damage to primary visual cortex (V1) demonstrate residual performance on laboratory visual tasks despite denial of conscious seeing (blindsight) [1]. After a period of recovery, which suggests a role for plasticity [2], visual sensitivity higher than chance is observed in humans and monkeys for simple luminance-defined stimuli, grating stimuli, moving gratings, and other stimuli [3–7]. Some residual cognitive processes including bottom-up attention and spatial memory have also been demonstrated [8–10]. To date, little is known about blindsight with natural stimuli and spontaneous visual behavior. In particular, is orienting attention toward salient stimuli during free viewing still possible? We used a computational saliency map model to analyze spontaneous eye movements of monkeys with blindsight from unilateral ablation of V1. Despite general deficits in gaze allocation, monkeys were significantly attracted to salient stimuli. The contribution of orientation features to salience was nearly abolished, whereas contributions of motion, intensity, and color features were preserved. Control experiments employing laboratory stimuli confirmed the free-viewing finding that lesioned monkeys retained color sensitivity. Our results show that attention guidance over complex natural scenes is preserved in the absence of V1, thereby directly challenging theories and models that crucially depend on V1 to compute the low-level visual features that guide attention.

Results and Discussion

Efficiently guiding attention toward the most relevant parts of the visual world is a higher visual function critical for survival, as supported by many theories of attention [11, 12]. In most theories and computational models, V1 is the central site where visual features are computed that guide attention toward salient locations [11–14]. Can blindsight patients or animals still compute such visual features? Although blindsight patients and animals exhibit significant residual visually guided behavior with simple laboratory tasks and stimuli, little is known quantitatively about their spontaneous natural vision (see [15, 16] for qualitative observations). Elucidating this question is important to understanding blindsight and the neural substrates of visual attention, and to possibly help affected patients better exploit residual visual processing in their daily life.

Macaque monkeys (n = 6) were trained to fixate and execute visually guided saccade tasks using simple stimuli. Primary visual cortex (V1) was then unilaterally removed in five monkeys by aspiration (as described previously [6]). Lesions covered at least 5°–20° in eccentricity and ±30° around the horizontal direction for all monkeys (see Figure S1A available online). After the lesion, the presence of residual vision was confirmed with visually guided saccade tasks, reported previously [6]. Here we examined spontaneous eye movements of these monkeys during free viewing of 164 natural movie clips (~70 min). Successful central fixation for 0.5 s triggered a movie clip (4.0–93.8 s/clip), presented either normally or horizontally flipped to eliminate stimulus-induced biases. Monkeys did not receive juice reward during free viewing; thus, movies were not associated with reward. 128,361 saccades were recorded (Figure 1A).

First, we examined whether the basic properties of free-viewing saccadic eye movements were affected by V1 lesion. With both normal and horizontally flipped movies, distributions of fixations on the absolute screen area exhibited no strong left-right bias, for both intact and lesioned monkeys (Figure 1B). Moreover, there was no significant difference in data from normal versus flipped movies (Figure 1C), which were thus merged for saliency analysis below. Polar histograms of relative saccade vector directions (Figure S1B) showed no obvious left-right bias that might have been induced by lesion (Figure S1C). However, lesion did affect movie viewing. When polar histograms of saccade vectors were restricted to only the first saccade of each movie clip, they were significantly biased away from the affected field (Figures S1D and S1E). Note that such bias did not affect the overall distribution of saccade vectors because the first saccades comprise only 1% of all saccades (820 out of 75,767). Intact monkeys did not exhibit such bias (Figure S1E). We also detected effects of lesion on distributions of saccade amplitude and of peak velocity (Figures S1F and S1G). These results are consistent with our previous reports using laboratory stimuli, in that V1 lesion affects saccade dynamics [6, 8, 17].

Taking these results together, our analysis of free-viewing eye movements demonstrated surprisingly little effect of V1 lesion: lesioned monkeys still made many saccades to targets in their affected field and explored the stimulus screen area thoroughly. However, they also exhibited clear sensory deficits, as shown by the first-saccade bias toward the intact field, which is in agreement with previous studies using laboratory stimuli [4, 6].

To better understand how guidance of gaze was affected by V1 lesion in natural free viewing, we employed a computational

[6]These authors contributed equally to this work
[7]Present address: Center for Neuroscience Studies, Queen's University, Kingston, ON K7L 3N6, Canada
[8]Present address: Laboratory for Adaptive Intelligence, RIKEN Brain Science Institute, Wako 351-0198, Japan
*Correspondence: itti@usc.edu

A

Category		Monkey's name	# of fixations
Intact monkey		H	21,891
		K	19,481
		U	11,222
Lesioned monkey	Left V1	A	11,849
		T	16,268
		G	13,568
	Right V1	H	23,029
		U	11,053

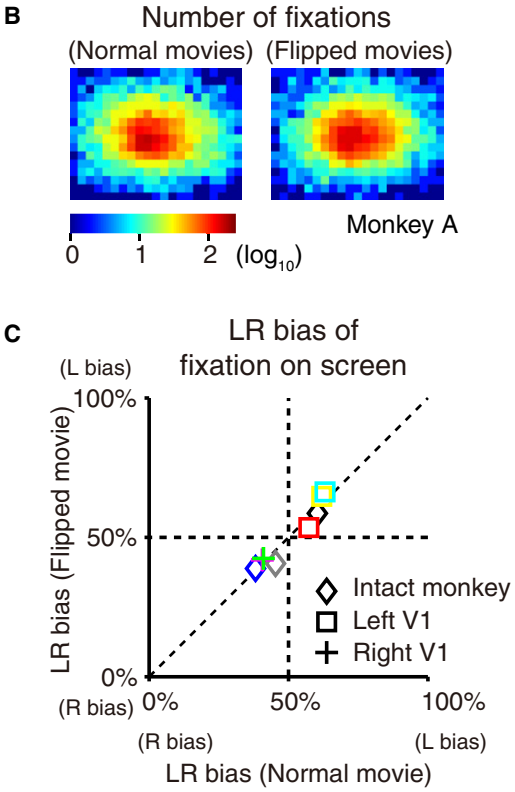

Figure 1. Basic Eye Movement Properties

(A) Number of saccades sampled in the free-viewing task for each of three monkey categories. In two monkeys (H and U), data were acquired both before and after lesion.

(B) Number of fixations on screen (monkey A) for normal (left) and horizontally flipped (right) presentations.

(C) Ratio of fixations on the left half of the screen to the total number of fixations (defined here as the LR bias) for normal movies (horizontal axis) versus horizontally flipped movies (vertical axis). Each symbol denotes data for a different monkey. The difference between the LR bias of normal movies and horizontally flipped movies was not significant ($p = 0.65$, paired t test, $n = 8$). See also Figure S1.

model of visual saliency to quantitatively titrate the nature of visual targets that monkeys looked at. Briefly, the saliency model [18, 19] decomposed incoming video inputs along several simple visual features at multiple spatial scales. Center-surround contrast operators for six center and surround scale combinations gave rise to feature maps that highlighted locations that differed from their neighbors in each feature. Finally, all feature maps were combined into a single saliency map to emphasize conspicuous visual locations in a feature-independent manner (Figure 2A). This model provides a flexible framework for predicting saliency maps from low-level feature maps, without necessarily committing to the exact origin or nature of the feature maps. Five features were used, each thought to contribute significantly to visual search in humans [20]: luminance, two chromatic contrasts (in the Derrington-Krauskopf-Lennie [DKL] color space derived from retinal ganglion cells [21]), orientation (V1-like Gabor filters in four orientations [22]), and motion (spatiotemporal energy model in four directions [23]). We quantified saliency-guided eye movements (Figure 2B) using receiver operating characteristic analysis of saliency values at endpoints of monkey saccades compared to random endpoints (Figure 2C) (see Figure S2 for random endpoint sampling scheme). This resulted in an area under the curve (AUC) score (0.5 indicates chance performance, i.e., eye movements are not guided by saliency, whereas the best expected score, from interobserver correlation analysis, might reach ~0.7; see Supplemental Experimental Procedures).

AUC scores were significantly above chance for all monkeys (Figure 2D), indicating that lesioned monkeys were still significantly attracted toward salient targets in their affected field. At the population level, V1 lesions significantly reduced but did not abolish the tendency of monkeys to gaze toward salient targets (intact monkeys: AUC = 0.627 ± 0.002; lesioned monkeys: AUC = 0.601 ± 0.003 in affected field, AUC = 0.627 ± 0.003 in normal field; see Figure 2D for statistical analysis). To investigate the possibility that some of the saccades into the affected field might be memory driven as opposed to truly visually guided, we duplicated the AUC analysis using only pure discovery saccades, i.e., saccades aimed toward screen locations that had never entered the intact field. The same pattern of results was observed (Figure S2C), excluding the possibility that memory was a dominant factor in directing saccades to the affected field.

Can we quantitatively explain differences in visual processing and saliency computations between normal and affected fields in term of features? To investigate this, we modified the model to examine relative contributions of the different basic features to gaze guidance. First, AUC scores were calculated for variants of the saliency model reduced to using only any one of our five features ("single-feature model"). All scores were significantly above chance, indicating that saliency in each feature taken separately still predicted monkey gaze above chance (Figure 3A). Because different features are often correlated in the natural visual world—e.g., a colorful object may also be brighter than the background, posing the question of whether color or brightness attracted attention (Figure 3B)—we sought to isolate the nonredundant contribution of each feature to saliency. To this end, we used an optimization procedure followed by a leave-one-feature-out approach (Supplemental Experimental Procedures). The optimization algorithm adjusted the weights of the five features to maximize the model's ability to predict monkey eye movements, separately for each of three different saccade groups (intact monkeys, affected field of lesioned monkeys, and normal field of lesioned monkeys, as defined in Figure 2D) (Figure S3). In the leave-one-feature-out approach, applied separately to each group, the AUC score of the optimized "full" model incorporating all features and the scores of each similarly optimized model incorporating all but one feature ("minus-one" model) were compared (Figure 3C). A nonredundant contribution index was defined as the AUC score difference between the full model and a reduced model divided

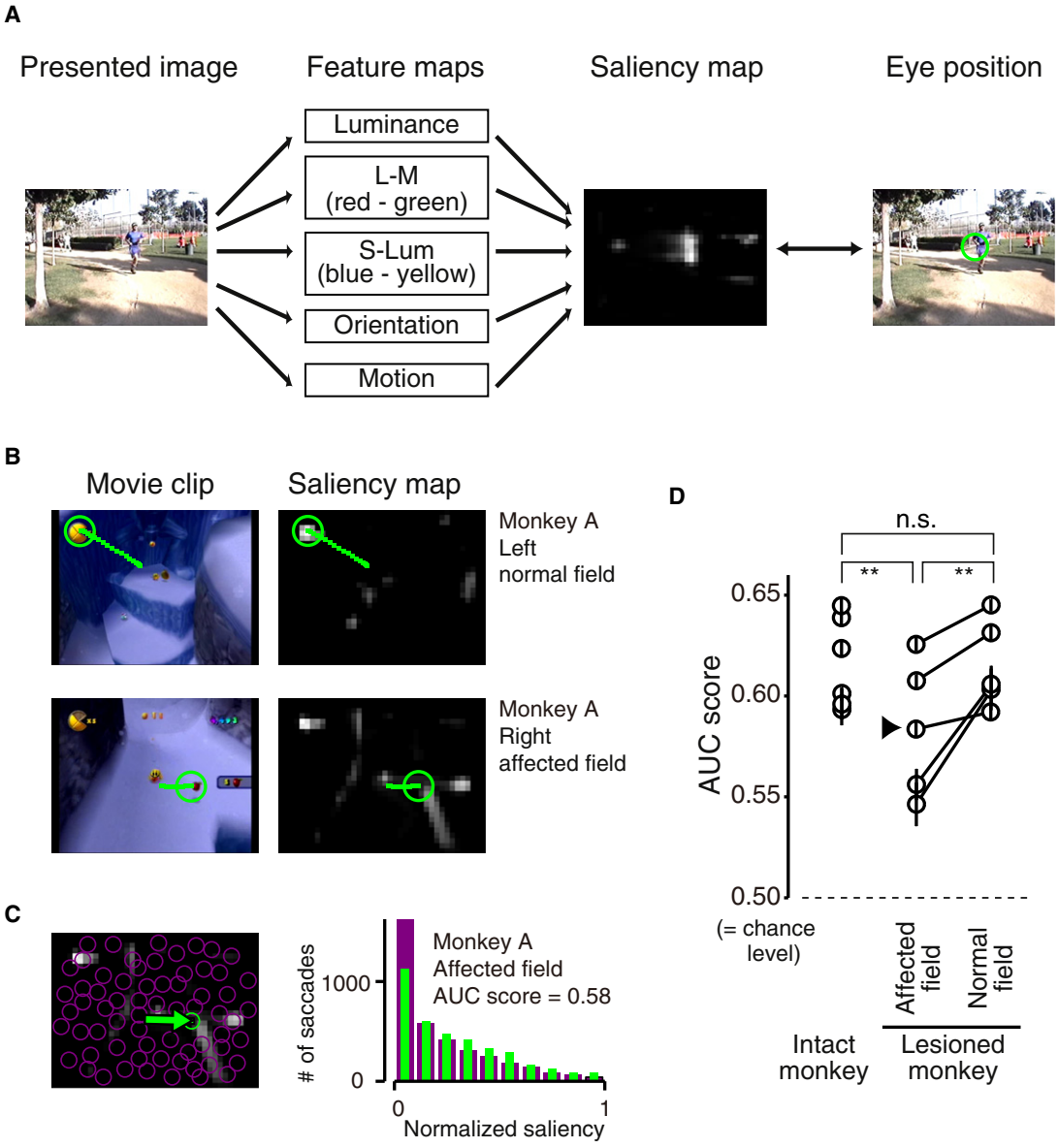

Figure 2. Residual Saliency-Guided Eye Movements after V1 Lesion

(A) Saliency model (see Supplemental Experimental Procedures for detailed definition of the features).

(B) Example movie frames (left) and saliency maps (right) with trajectory of an eye movement. Top: first saccade of a normally presented movie clip (movie 003, frame 5) directed leftward (normal field), toward a salient colorful object. Bottom: 91st saccade of the same clip (frame 1243) directed rightward (affected field), toward a salient moving object.

(C) Quantitative analysis of saliency-guided eye movements. Saliency values at each monkey saccade endpoint (green) and for random endpoints (magenta) were sampled (left) and histogrammed (right). Receiver operating characteristic analysis of the histograms yielded an area under the curve (AUC) score. AUC scores were computed separately for leftward and rightward saccades.

(D) AUC scores for three groups: "intact monkey," data for left and right directions (six hemifields) for the three intact monkeys; "affected field" and "normal field," data for the five lesioned monkeys. Error bars indicate SE. In all cases, AUC scores were significantly above chance (0.5) ($p < 0.05$, two-tailed t test). In group comparisons, ** indicates significant group mean difference ($p < 10^{-9}$, Wilcoxon signed-rank test after Bonferroni correction); n.s. indicates not significant ($p > 0.10$, Wilcoxon signed-rank test after Bonferroni correction).

See Figure S2 for consideration of sampling scheme.

by the AUC score of the full model minus 0.5 (Figure 3C). The index reflects how much a particular feature contributed to gaze guidance, beyond what could already be explained by the other four features. Figure 3D summarizes the contribution indices obtained. The pattern of feature contributions in intact monkeys resembled that in the normal field of lesioned monkeys (Spearman's rank partial correlation $r = 0.90$, $p = 0.09$, $n = 5$), in which the contribution of motion is highest and those of color, orientation, and luminance follow (in decreasing order). After V1 lesion, however, that order shifted to motion, luminance, color, and orientation. This pattern did not resemble others ($r = 0.55$, $p > 0.2$ for affected field of lesioned monkeys versus intact monkeys; $r = -0.39$, $p > 0.2$ for affected field versus normal field of lesioned monkeys;

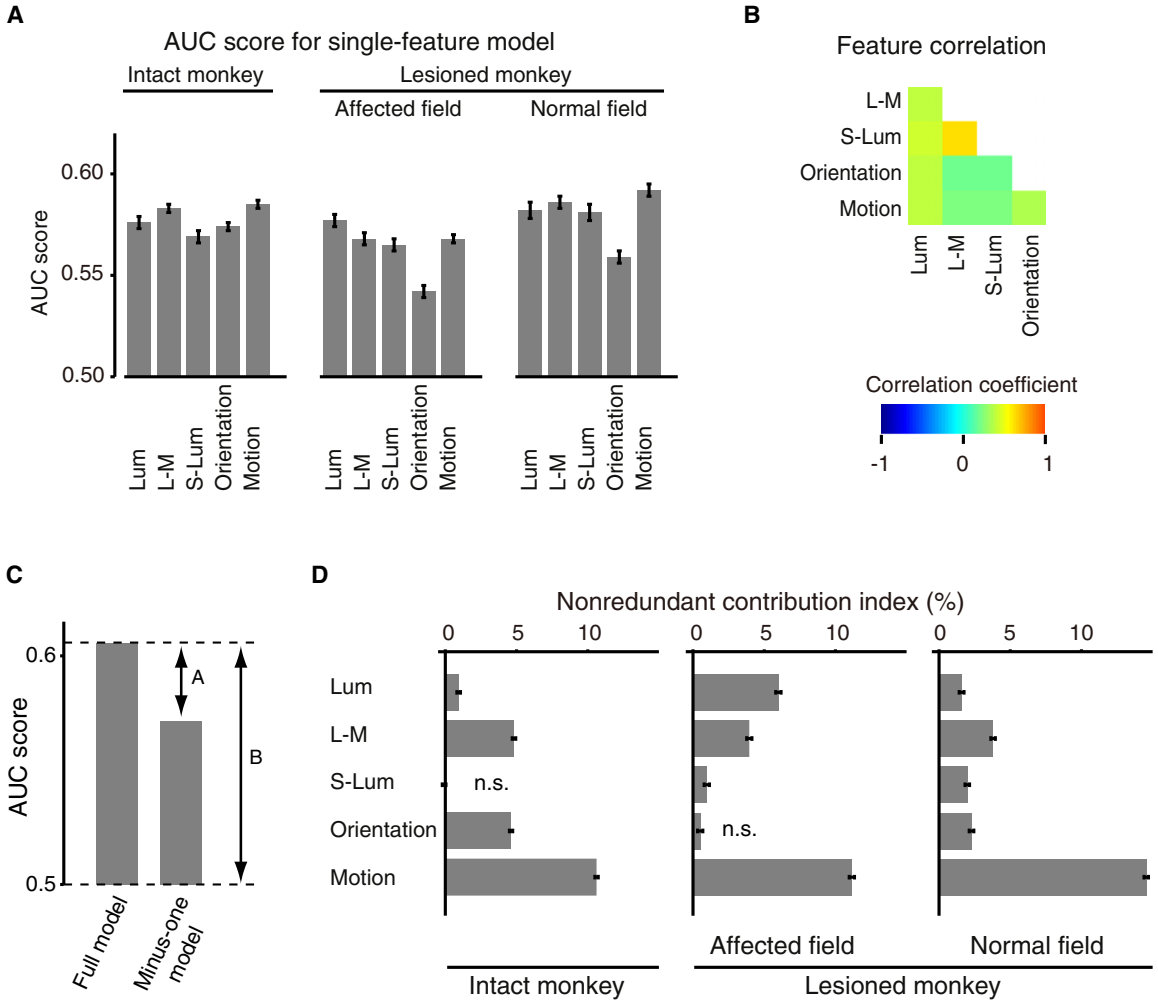

Figure 3. Contribution of Saliency for Each Feature

(A) AUC scores for single-feature models, for three groups as in Figure 2D, were all significantly above chance (0.5) ($p < 0.05$, two-tailed t test). Error bars indicate SE. Feature channels are as in Figure 2A. "Lum" denotes the luminance channel.

(B) Correlation coefficients between features over all movie frames used in the experiments were all significantly higher than zero ($p < 10^{-9}$ after Bonferroni correction).

(C) Variable-weight model. An optimized full model with all features was compared with a leave-one-feature-out model lacking one feature ("minus-one model"). The resulting differences between AUC scores (arrow A) were divided by the AUC score of the full model minus 0.5 (arrow B), which was used to define the nonredundant contribution index of the feature of interest (here, motion).

(D) Nonredundant contribution index of each feature (0 indicates that the feature of interest did not contribute to gaze guidance in any unique manner beyond what the other four features could predict). All of the feature contributions, except for those indicated n.s. (not significant), were significantly higher than zero ($p < 0.05$, paired t test, with Bonferroni correction for 15 simultaneous tests). Note that the contribution index does not add up to 100% (by definition). Error bars indicate SE.

Spearman's rank partial correlation). Our analysis thus shows an interesting pattern of differences between intact and lesioned monkeys (Figure 3D): the contribution of orientation was decreased, luminance was increased, and motion and color remained relatively unchanged (see also the section "Consideration of Previous Results" in the Supplemental Information).

In Figure 3D, the finding that the contribution of color was not abolished in the affected field was surprising given contrasting results from previous laboratory experiments [3, 24–26]. This may be specific to our natural free-viewing paradigm. Hence, we designed a control laboratory experiment to verify the model's prediction.

Two lesioned monkeys were tested with a visually guided saccade task using equiluminant chromatic stimuli (Figure 4A). Lesioned monkeys detected, above chance, two types of equiluminant chromatic stimuli tuned to different ganglion cell types (Figure 4B). Although performance with chromatic stimuli was below that with high-contrast achromatic stimuli (positive control, confirming residual vision for luminance-defined shapes), it was better than for low-contrast achromatic stimuli (negative control, indicating that slight luminance differences between chromatic stimuli and background are unlikely to have contaminated chromatic processing). This was further confirmed in one monkey for a range of slight luminance variations (Figure 4C; see figure legend for detail). We further tested the monkey with color detection tasks using either mosaic stimuli or colored Gaussian stimuli to exclude possible contributions of edge artifacts and luminance differences (Figure S4). In sum, our

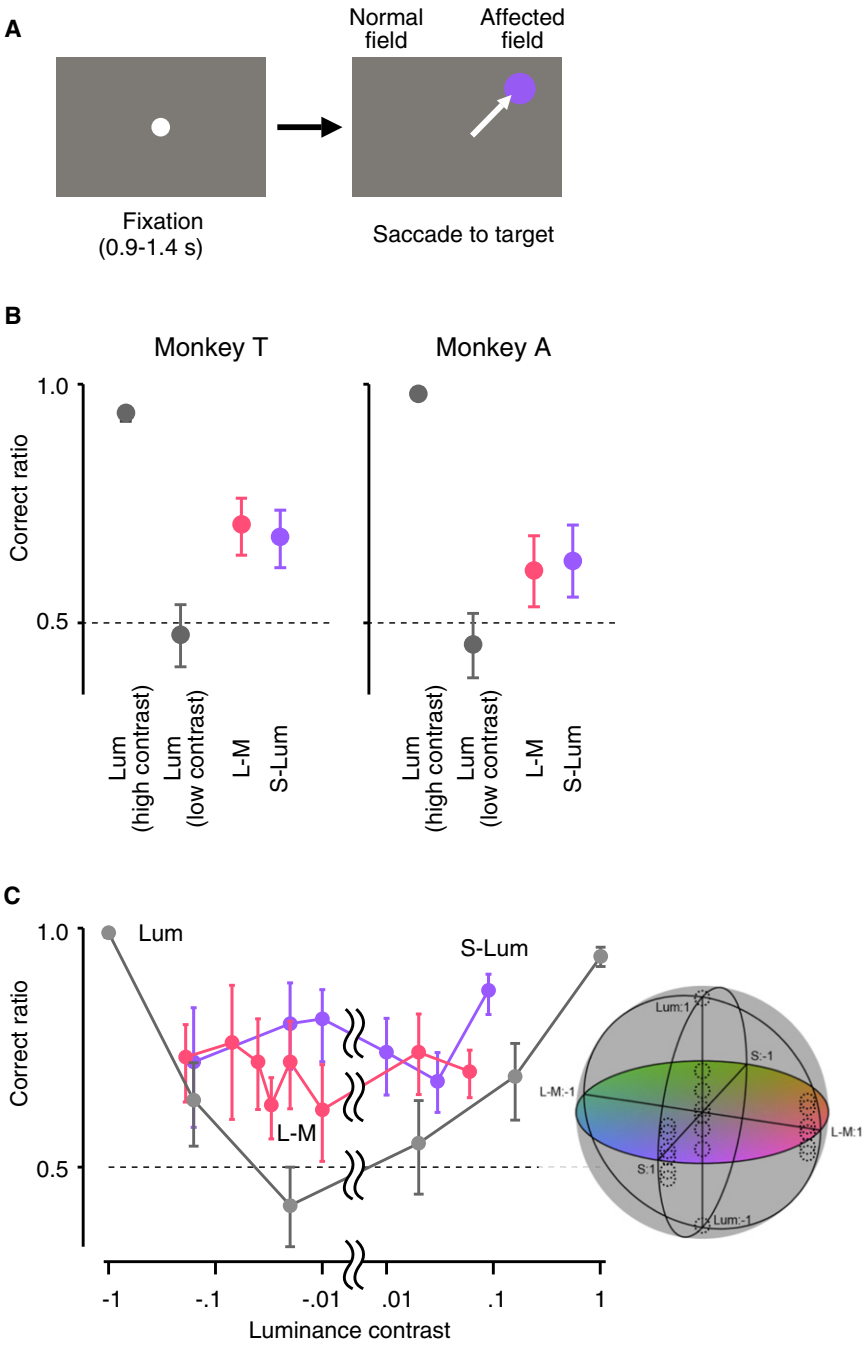

Figure 4. Direct Evaluation of Residual Chromatic Processing after V1 Lesion

(A) Visually guided saccade task using equiluminant chromatic stimuli. A single target stimulus was presented in the affected hemifield, either above or below the horizontal meridian. Correct forced-choice saccade to the target yielded fruit juice reward. Performance was evaluated by calculating the correct ratio as the number of trials with saccades toward the same quadrant as the target stimulus divided by the total number of trials with successful fixation before stimulus presentation.

(B) Performance for two lesioned monkeys (T and A). Lum (high contrast), achromatic stimuli with a luminance contrast of 2.3; Lum (low contrast), achromatic stimuli with a luminance contrast of 0.02 and −0.02 for monkey T and 0.04 and −0.04 for monkey A; L-M, equiluminant chromatic stimuli with isolated L-M channel stimulation; S-Lum, equiluminant chromatic stimuli with isolated S-Lum channel stimulation. Error bars denote 95% confidence interval. For Lum (high contrast), L-M, and S-Lum, but not for Lum (low contrast), performance was significantly above chance (0.5).

(C) Correct ratio for stimuli with small luminance difference added (horizontal axis) to account for possible contribution of deviations from exact equiluminance. Color coding is as in (B). Error bars denote 95% confidence interval. Data for monkey T are shown. Correct ratio remained significantly above chance for chromatic stimuli even over the range where it dropped to chance for luminance-defined stimuli, hence confirming that observed performance with chromatic stimuli was not due to contamination from luminance. Right: parameter of stimuli used in this experiment is depicted as dotted circles in the Derrington-Krauskopf-Lennie (DKL) color space.

control experiments using simple stimuli directly confirm residual guidance toward purely chromatic information, as predicted by our saliency model and free-viewing experiment. More broadly, color information was hence used during both forced-choice and spontaneous behavior in our blindsight animals.

In summary, for the first time, using a computational saliency model together with eye movement recording during free viewing of natural video stimuli, we observed sophisticated gaze orienting toward salient stimuli in blindsight. Our approach, combining computational modeling and free viewing, successfully allowed us to titrate the impact of V1 lesions on processing of visual features and the spontaneous guidance of attention. Our results complement and extend previous laboratory experiments in a manner that is more relevant to daily life. It should be emphasized that our experiments and results concern detection and attention/gaze guidance, but not discrimination or identification. Thus, when we find that monkeys look toward stimuli in their affected field that are salient, e.g., in the color domain, this does not necessarily imply that the monkeys are capable of identifying or discriminating colors (see Supplemental Information).

Our study clearly shows that, after recovery, there is more to visual attention and saliency than the pathway through V1. We succeeded in pinpointing the features that guide residual vision, by expanding our original computational model to allow differential contributions of visual features. We believe that the use of natural movie stimuli is an important feature of the present study that places our results into a context more relevant to everyday life [27]. An important question for future research is whether the attention processes that we have shown to be active in postrecovery blindsight also contribute significantly to saliency, attention, and gaze even

in the normal brain. Our study also shows that computational models of attention cannot rely exclusively on V1 as the primary center for saliency computation [13], and that they should also consider how alternate pathways may provide critical feature information to the primate attention and saliency mechanisms.

Experimental Procedures

Six Japanese monkeys (*Macaca fuscata*; three male and three female, body weight 5–9 kg) were implanted with scleral search coils and a head holder (see Supplemental Experimental Procedures). All experimental procedures were performed in accordance with the National Institutes of Health Guidelines for the Care and Use of Laboratory Animals and were approved by the Committee for Animal Experiment at the National Institutes of Natural Sciences. After pretraining, V1 was surgically removed by aspiration under anesthesia in five monkeys. Free-viewing task was performed 15, 9, 28, 9, and 19 months after V1 lesion for monkeys A, H, T, U, and G, respectively. As a control, monkeys H and U were also tested before lesion, and intact monkey K was also tested. Monkeys watched 164 video clips that varied in duration and semantic content. Saccadic eye movements were determined using an algorithm that combined smoothed velocity measurements with a windowed principal components analysis [18]. A validated computational model of visual attention was used to predict individual eye movements (Figure 2A) [14, 19]. Two lesioned monkeys (T and A) were also tested with a visually guided saccade task with equiluminant color stimuli. Target stimuli were circular spots whose color properties were derived from the DKL color space [21].

Supplemental Information

Supplemental Information includes four figures and Supplemental Experimental Procedures and can be found with this article online at doi:10.1016/j.cub.2012.05.046.

Acknowledgments

This work was supported by the Human Frontier Science Program, the National Science Foundation, the Army Research Office, the Defense Advanced Research Projects Agency, Grants-in-Aid for Scientific Research (KAKENHI; 21500377 and 22220006), the Core Research for Evolutionary Science and Technology program of the Japan Science and Technology Agency, and the Excellent Young Researchers Overseas Visit Program of the Japan Society for the Promotion of Science. The views, opinions, and findings contained in this article are those of the authors and should not be interpreted as representing the official views or policies, either expressed or implied, of the Defense Advanced Research Projects Agency or the Department of Defense.

Received: March 18, 2012
Revised: May 1, 2012
Accepted: May 23, 2012
Published online: June 28, 2012

References

1. Weiskrantz, L. (1986). Blindsight: A Case Study and Implications (Oxford: Clarendon Press).
2. Payne, B.R., and Lomber, S.G. (2001). Reconstructing functional systems after lesions of cerebral cortex. Nat. Rev. Neurosci. *2*, 911–919.
3. Cowey, A., and Stoerig, P. (2001). Detection and discrimination of chromatic targets in hemianopic macaque monkeys and humans. Eur. J. Neurosci. *14*, 1320–1330.
4. Moore, T., Rodman, H.R., Repp, A.B., and Gross, C.G. (1995). Localization of visual stimuli after striate cortex damage in monkeys: parallels with human blindsight. Proc. Natl. Acad. Sci. USA *92*, 8215–8218.
5. Weiskrantz, L., Barbur, J.L., and Sahraie, A. (1995). Parameters affecting conscious versus unconscious visual discrimination with damage to the visual cortex (V1). Proc. Natl. Acad. Sci. USA *92*, 6122–6126.
6. Yoshida, M., Takaura, K., Kato, R., Ikeda, T., and Isa, T. (2008). Striate cortical lesions affect deliberate decision and control of saccade: implication for blindsight. J. Neurosci. *28*, 10517–10530.
7. Kato, R., Takaura, K., Ikeda, T., Yoshida, M., and Isa, T. (2011). Contribution of the retino-tectal pathway to visually guided saccades after lesion of the primary visual cortex in monkeys. Eur. J. Neurosci. *33*, 1952–1960.
8. Ikeda, T., Yoshida, M., and Isa, T. (2011). Lesion of primary visual cortex in monkey impairs the inhibitory but not the facilitatory cueing effect on saccade. J. Cogn. Neurosci. *23*, 1160–1169.
9. Kentridge, R.W., Heywood, C.A., and Weiskrantz, L. (1999). Attention without awareness in blindsight. Proc. Biol. Sci. *266*, 1805–1811.
10. Takaura, K., Yoshida, M., and Isa, T. (2011). Neural substrate of spatial memory in the superior colliculus after damage to the primary visual cortex. J. Neurosci. *31*, 4233–4241.
11. Koch, C., and Ullman, S. (1985). Shifts in selective visual attention: towards the underlying neural circuitry. Hum. Neurobiol. *4*, 219–227.
12. Treisman, A.M., and Gelade, G. (1980). A feature-integration theory of attention. Cognit. Psychol. *12*, 97–136.
13. Li, Z. (2002). A saliency map in primary visual cortex. Trends Cogn. Sci. *6*, 9–16.
14. Itti, L., Koch, C., and Niebur, E. (1998). A model of saliency-based visual attention for rapid scene analysis. IEEE T. Pattern Anal. *20*, 1254–1259.
15. Humphrey, N.K. (1974). Vision in a monkey without striate cortex: a case study. Perception *3*, 241–255.
16. de Gelder, B., Tamietto, M., van Boxtel, G., Goebel, R., Sahraie, A., van den Stock, J., Stienen, B.M., Weiskrantz, L., and Pegna, A. (2008). Intact navigation skills after bilateral loss of striate cortex. Curr. Biol. *18*, R1128–R1129.
17. Isa, T., and Yoshida, M. (2009). Saccade control after V1 lesion revisited. Curr. Opin. Neurobiol. *19*, 608–614.
18. Berg, D.J., Boehnke, S.E., Marino, R.A., Munoz, D.P., and Itti, L. (2009). Free viewing of dynamic stimuli by humans and monkeys. J. Vis. *9*, 1–15.
19. Itti, L., and Koch, C. (2001). Computational modelling of visual attention. Nat. Rev. Neurosci. *2*, 194–203.
20. Wolfe, J.M., and Horowitz, T.S. (2004). What attributes guide the deployment of visual attention and how do they do it? Nat. Rev. Neurosci. *5*, 495–501.
21. Derrington, A.M., Krauskopf, J., and Lennie, P. (1984). Chromatic mechanisms in lateral geniculate nucleus of macaque. J. Physiol. *357*, 241–265.
22. Daugman, J.G. (1980). Two-dimensional spectral analysis of cortical receptive field profiles. Vision Res. *20*, 847–856.
23. Adelson, E.H., and Bergen, J.R. (1985). Spatiotemporal energy models for the perception of motion. J. Opt. Soc. Am. A *2*, 284–299.
24. Brent, P.J., Kennard, C., and Ruddock, K.H. (1994). Residual colour vision in a human hemianope: spectral responses and colour discrimination. Proc. Biol. Sci. *256*, 219–225.
25. Leh, S.E., Mullen, K.T., and Ptito, A. (2006). Absence of S-cone input in human blindsight following hemispherectomy. Eur. J. Neurosci. *24*, 2954–2960.
26. Tamietto, M., Cauda, F., Corazzini, L.L., Savazzi, S., Marzi, C.A., Goebel, R., Weiskrantz, L., and de Gelder, B. (2010). Collicular vision guides nonconscious behavior. J. Cogn. Neurosci. *22*, 888–902.
27. Nardo, D., Santangelo, V., and Macaluso, E. (2011). Stimulus-driven orienting of visuo-spatial attention in complex dynamic environments. Neuron *69*, 1015–1028.